

Sequential Distribution Analysis of Metabolites in Blue Morning Glory (*Ipomoea indica*) Petals by Matrix Assisted Laser Desorption/Ionization Time-of-Flight Mass Spectrometry

Hideyuki Kajiwara^{1*} and Akemi Shimizu²¹Advanced Analysis Center, National Agriculture and Food Research Organization, Tsukuba, Ibaraki 305-8517, Japan²Institute of Crop Science, National Agriculture and Food Research Organization, Hitachiomiya, Ibaraki 319-2293, Japan

Abstract

Blue morning glory (*Ipomoea indica*) has a color gradient on its petals that change during flowering. Although anthocyanins were thought to be responsible for the color variations among varieties, their distribution and metabolite changes in petals that might be affected by anthocyanins color during flowering were not clear. The petals were analyzed by matrix assisted laser desorption/ionization time-of-flight mass spectrometry. Metabolites extracted from sequential disc cut samples from petal tissue showed that the metabolites, including anthocyanins, were not uniformly distributed in petals and their distribution changed during flowering

Keywords: Anthocyanin; Biotyping; Blue morning glory (*Ipomoea indica*); Matrix assisted laser desorption/ionization time-of-flight mass spectrometry (MALDI-TOF MS); Metabolite; Petal

Introduction

Perennial blue morning glory (BMG) (*Ipomoea indica*), which belongs to the same genus as annual Japanese morning glory (*I. nil*), morning glory (*I. tricolor*), common morning glory (*I. purpurea*), and fence morning glory (*I. ochracea*), has funnel-shaped flower petals with blue color gradients. The flowers open in the morning and then shrink till evening, changing the petal colors. Anthocyanins were considered as the most important factor for petal color, and pH changes inside the petal cells were thought to cause changes in flower color. *Pr* gene products in *I. tricolor* are responsible for pH changes in petal cells [1-4]. However, it is unknown what kinds of metabolites in BMG petals change during flowering.

Recently, BMG for green sun shades are being sold, and the commercial need to discriminate between varieties has increased. Many trade names have been observed in the market, and some could not be distinguished. It was guessed that nursery plants obtained by herbaceous cutting were sold under different commercial names. However, there was no rapid method for the discrimination of BMG varieties. While there is no BMG genome information, the whole genome for *I. nil* has been decoded [5]. As far as we know, there was no report of randomly amplified polymorphic DNA analysis in BMG. If whole genome information of specific BMG varieties was known, then genomic differences, including single nucleotide polymorphism among varieties, would allow for the discrimination between varieties, such as BMG radiation-induced mutant cv. Capetown Sky (registered name: IRBli Light Blue) [6].

Matrix assisted laser desorption/ionization time-of-flight mass spectrometry (MALDI-TOF MS) has been applied to analyze biological samples. MALDI biotyping has been applied to discriminate between species of bacteria, fungi, and small pests by measuring the mass range from *m/z* 2000 to 20000 [7-9]. In flowers, the fingerprints obtained from petals were considered as candidates for the rapid discrimination of varieties because the metabolites, including anthocyanins, were specific in each variety. If petal metabolites change depending on environmental conditions [10], petal metabolites are relatively stable during flowering rather than the leaves and stems that have age gradients and tissue differentiations. Furthermore, MALDI-TOF MS imaging is starting to be applied as a method for tissue analysis [11]. Although most reports concerned animal tissues using thin sliced sections, the number of

reports that used imaging analyses for plant tissues has been increasing [12-14]. As far as we know, there is no imaging analysis available for petals, except for those in *Arabidopsis* that used a hybrid linear ion trap-orbitrap mass spectrometer [15].

We analyzed BMG petals using MALDI-TOF MS and investigated the sequential distributions of metabolites including anthocyanins for three days, from one day before flowering (1DBF) to one day after flowering (1DAF). The ultimate aim was to provide a rapid and costless discrimination of BMG varieties using petals like that of MALDI biotyping of bacteria [7,8] and small insects [9] in future.

Materials and Methods

Chemicals

Trifluoroacetic acid and hydrochloric acid (HCl) were purchased from Nacalai Tesque, Kyoto, Japan. Acetonitrile and ethanol were obtained from Wako Pure Chemical Industries, Osaka, Japan and α -cyano-4-hydroxycinnamic acid (CCA) was from Sigma-Aldrich, St. Louis MO, USA. A peptide calibration standard (Bruker Daltonics, Billerica MA, USA) was used for the calibration.

Cultivation and sampling

Potted BMG (*I. indica* cv. Capetown Blue) were cultivated at the National Agriculture and Food Research Organization.

Double-sided carbon tape (cat. 7314, Nisshin EM Co., Tokyo, Japan) was placed on the MALDI-TOF MS target (Bruker Daltonics). The abaxial side of the petal was bound to carbon tape (Figure 1). One microliter of ethanol containing 1% HCl was manually spotted onto the petal and it was left at room temperature until the dehydration of

*Corresponding author: Hideyuki Kajiwara, Advanced Analysis Center, National Agriculture and Food Research Organization, Tsukuba, Ibaraki 305-8517, Japan, Tel: +81298387900; E-mail: kajiwara@affrc.go.jp

Received December 06, 2017; Accepted December 12, 2017; Published December 18, 2017

Citation: Kajiwara H, Shimizu A (2017) Sequential Distribution Analysis of Metabolites in Blue Morning Glory (*Ipomoea indica*) Petals by Matrix Assisted Laser Desorption/Ionization Time-of-Flight Mass Spectrometry. Mass Spectrom Purif Tech 3: 121. doi:10.4172/2469-9861.1000121

Copyright: © 2017 Kajiwara H, et al. This is an open-access article distributed under the terms of the Creative Commons Attribution License, which permits unrestricted use, distribution, and reproduction in any medium, provided the original author and source are credited.

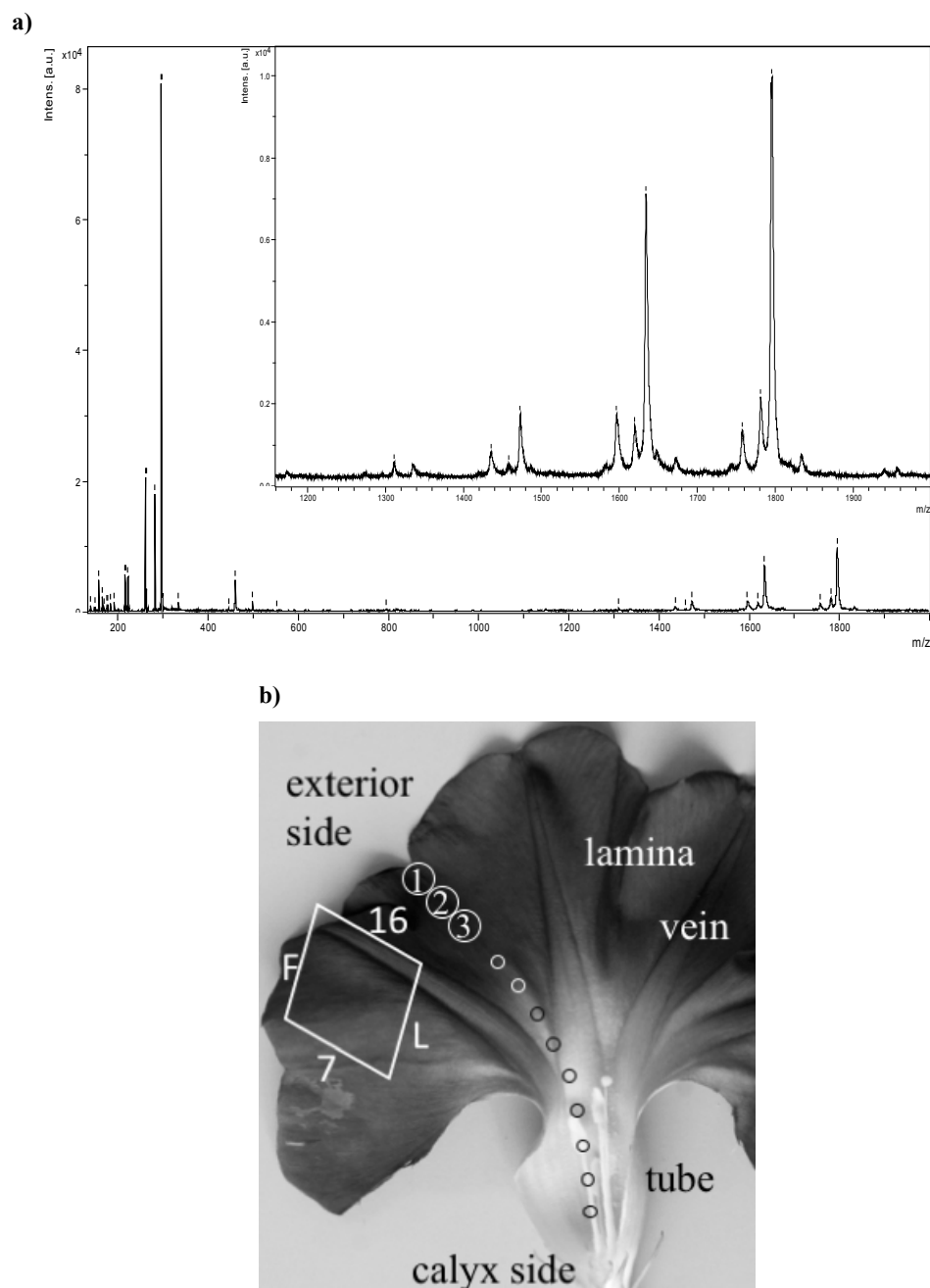


Figure 1: a) MALDI-TOF MS analysis of flower petals on double-sided carbon tape. Mass fingerprints of petals at position F10 on MALDI is shown. b) The schematic sampling image for MALDI-TOF MS analyses, the disc samples using a circle cutter is illustrated using a dissected BMG flower.

the solution. The same volume of CCA saturated in acetonitrile: water: trifluoroacetic acid (50:47.5:2.5) was spotted on the same position and the petal was then dried in a vacuum.

Discs were sequentially cut from petals from the center of the lamina between the veins and from the exterior side to calyx side using a circle cutter (5 mm diameter, Takasho Gimune MFG Co. Ltd., Hyogo, Japan) and numbered (Figure 1). The discs were then ground with 20 μ L of ethanol containing 1% HCl in a tube. Extracts obtained by centrifugation at 15000 rpm for 5 min at 4°C were spotted on 384 stainless MALDI-TOF MS targets, and the same volume (0.5 μ L) of

CCA solution was immediately added to the solution for analysis. Extracted samples were stored at -20°C until use.

MALDI-TOF MS analysis and data analysis

The Autoflex III instrument (Bruker Daltonics) was used in a linear positive mode. Ions were generated by a 100 Hz Nd:YAG laser. Each spectrum resulted from 100 laser shots at 10 random positions within the spots. Mass spectra were generated in the mass range m/z 140–2000. Mass spectra were analyzed by Flex Analysis 2.0 and Microsoft Excel 2007. Each peak intensity was added to provide the sum of all peak

intensities. The peak percent of each peak was then calculated as peak intensity divided by the sum of all peak intensities. Factors based on the petal length ratio were used to compensate for different petal radii.

Results and Discussion

Mass spectrometry of petals

For the initial analysis of BMG petals, MALDI-TOF MS was used from m/z 2000 to 20000 in both linear and reflector modes (Data not shown). This analysis range was used for the discrimination of bacteria and fungi to analyze protein mass fingerprints [7-9]. The observed peaks were considered species-specific ribosomal proteins and other major proteins in MALDI biotyping. However, there was no obvious peak in petal extracts in this range so the mass range used for the identification of microorganisms could not use for the discrimination of varieties using BMG petals.

Mass fingerprints of the exterior blue part of petals are shown (Figure 1). Petals are relatively thin so we tried a direct petal analysis. For this purpose, petals were placed on double-sided carbon tape to liberate static electricity instead of a gold-coated glass slide because petals were too large. Approximately one-third of the whole petal was placed on the carbon tape. Although the calibration standard was placed directly on the carbon tape, there were still differences in the vertical distances between the mass standards and metabolites on the

tissue because of the thickness of the petal. However, the resolution of the direct MALDI-TOF MS analysis was not high (Data not shown). If better MALDI-TOF MS apparatus ex. the orbitrap and program were available, metabolite distribution could be visualized in a better image resolution and this could be used for a detailed sequential analysis of metabolite distribution in petals.

High mass peaks within the range $>m/z$ 1000 were considered to be glycosylated anthocyanins (Figure 1, inset). There were approximately 161 mass differences between the peaks observed at m/z 1311, m/z 1472, m/z 1633, and m/z 1794. The mass differences were presumed to come from glycosylation. Heavenly blue anthocyanin, a glycosylated anthocyanin isolated from the *I. tricolor* cv. Heavenly Blue, had a molecular weight of 1760.5 [16]. The anthocyanins observed in BMG were different from heavenly blue anthocyanin, which was identified as the *I. tricolor* cv. Heavenly Blue. Identification of BMG anthocyanins remains to be studied further.

Sequential petal disc analysis

All of the 54 observed peaks were picked up and their peak intensities were measured. Peaks of different samples could not be compared directly by their differences in peak intensity. To cancel out sample differences, the peak percent of each peak was calculated. Each peak intensity was divided by the sum of all peak intensities and the results are illustrated in Figures 2 and 3 (Appendix Figure). Peak ratios

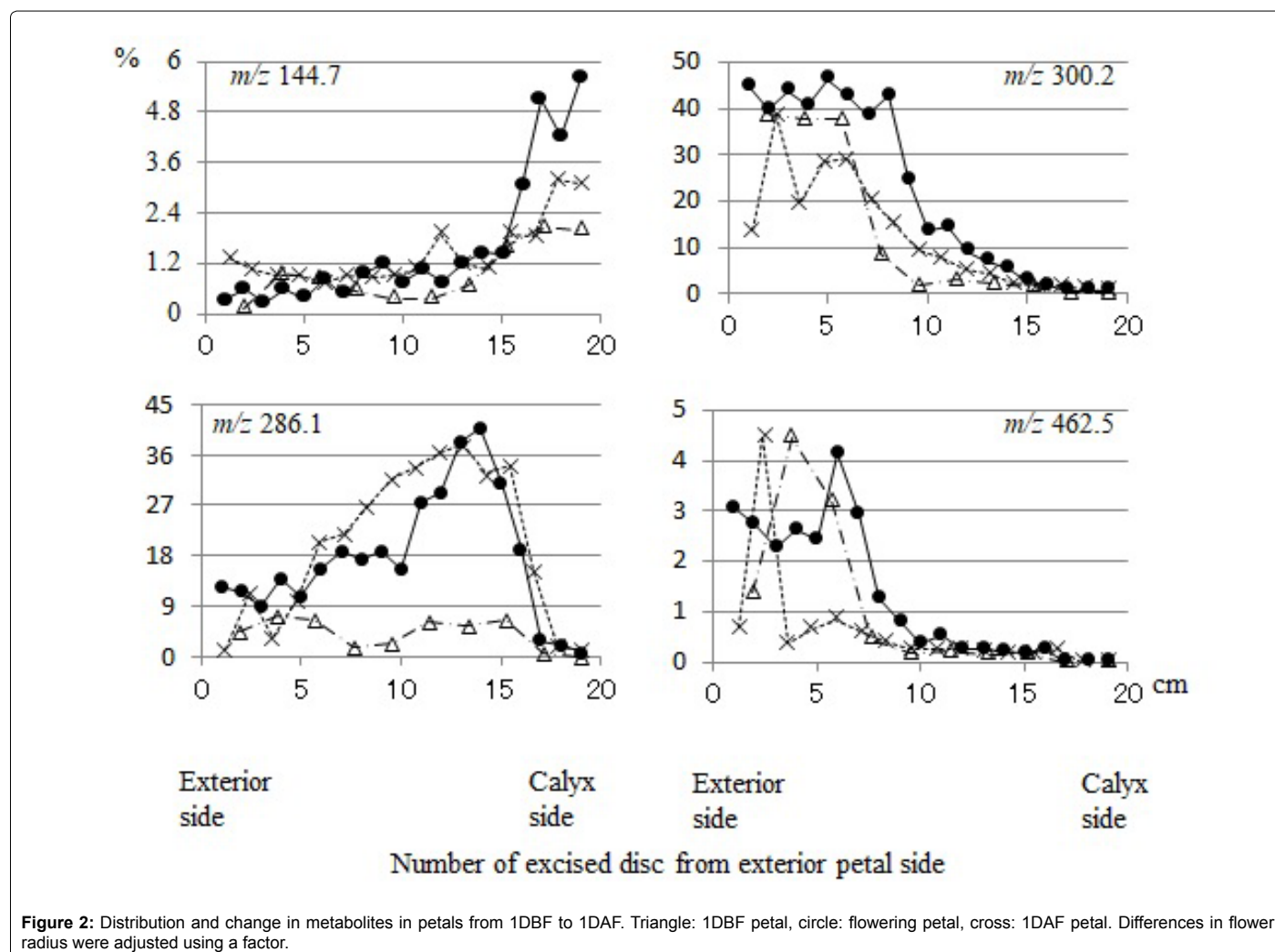


Figure 2: Distribution and change in metabolites in petals from 1DBF to 1DAF. Triangle: 1DBF petal, circle: flowering petal, cross: 1DAF petal. Differences in flower radius were adjusted using a factor.

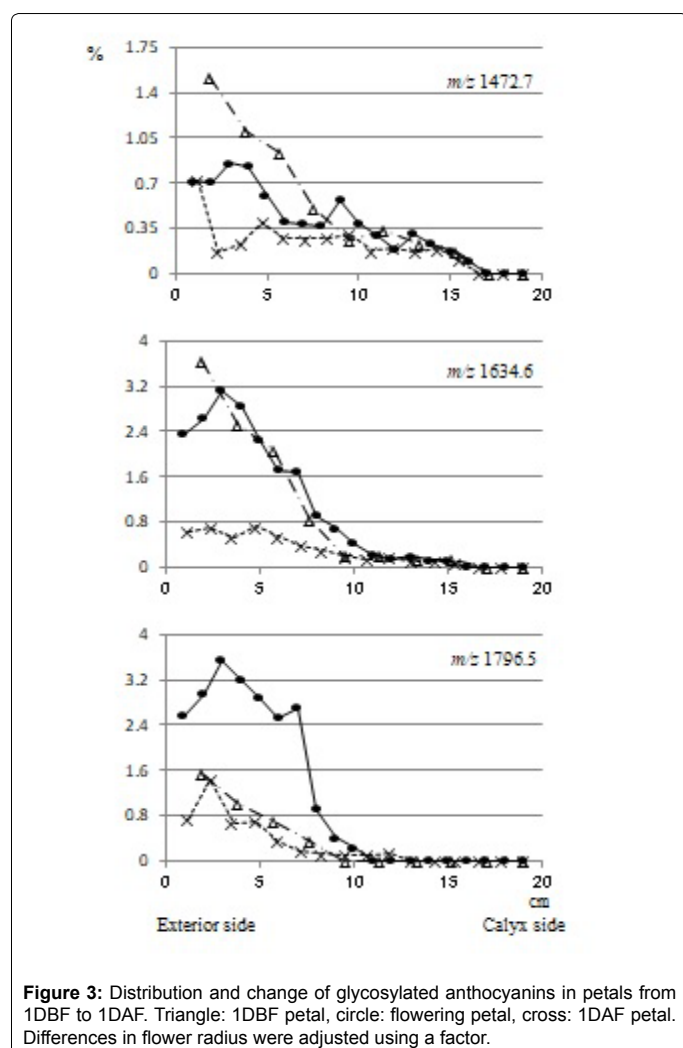


Figure 3: Distribution and change of glycosylated anthocyanins in petals from 1DBF to 1DAF. Triangle: 1DBF petal, circle: flowering petal, cross: 1DAF petal. Differences in flower radius were adjusted using a factor.

were also calculated; each peak height was divided by the highest peak (data not shown) and peak ratios were basically the same as percentage data.

While petal size changed during flowering, there was also a difference in flower size, and factors were used to compensate for differences in flower radii. Nineteen disc samples were obtained from flowering BMG. A total of 10 and 16 disc samples were obtained from 1DBF and 1DAF petals, respectively. 1DBF petals were smaller than flowering petals, and the size-adjustment factor was calculated as 1.90. For 1DAF petals that shrank in the evening and were smaller than flowering petals, the factor was 1.19. A comparison of the three size-adjusted samples is shown in Figures 2 and 3 (Appendix Figure). A total of 54 peaks were observed in BMG petals from 1DBF to 1DAF.

The peak percent observed at m/z 144.7 was increasingly distributed from the exterior side to the interior side (Figure 2). This tendency was the same for 1DBF and 1DAF of petals. This substance was considered to exist at almost the same amount in petals over 3 days. No transportation and no chemical reaction occurred on this metabolite. On the other hand, the metabolite observed at m/z 300.2 gradually decreased from the exterior side to the interior side (Figure 2). This tendency did not change from 1DBF to 1DAF. This metabolite was also considered to exist in almost the same amount over 3 days but their gradients in petals were different.

The peak at m/z 286.1 was scarcely observed in 1DBF petals (Figure 2). This peak became prominent in flowering petals compared to other metabolites, accounting for more than 36%. This metabolite was considered to be distributed in the basal part of a petal but not in the area that touched the calyx. It was also considered to synthesize in the petal during flowering, or it was transported from outside the petal. The peak at m/z 302.2 showed the same tendencies as m/z 286.1 (Appendix Figure). Conversely, the peak at m/z 264.9 decreased after flowering and was then distributed in almost same the amount in every part of the petal (Appendix Figure). Water flow in petals moved from the calyx part to the exterior part during flowering and water disappeared from petals by evaporation during fading, thus, sequential metabolite distributions were complicated and vicissitudes were unidirectional. Although our study ultimate objective was to develop a rapid and costless discrimination method of BMG varieties based on differences in mass fingerprints of petal metabolites, we did not anticipate dynamic changes in metabolites over 3 days of flowering.

The peaks at m/z 1472.7, m/z 1634.6, and m/z 1796.5, which had 161.9 intervals, were considered to be glycosylated anthocyanins (Figure 3). These showed a higher peak percent in the exterior side compared with that in the calyx side of petals. The peak observed at m/z 1472.7 showed a higher peak percent at 1DBF, the scores then decreased with flowering. The peak percent observed at m/z 1634.6 was almost the same as that at 1DBF and during flowering. The peak percent of m/z 1796.5 was at a maximum during flowering. Although these three peaks were presumed to be glycosylated anthocyanins that differ based on their glycosylated residue, their chronological behaviors were different from each other in detail.

A difference of molecular weight 161 between the peaks meant that the glycosylated metabolite peaks observed at m/z 1457.8 and m/z 1618.9 had a difference of 161.1. Durbin et al. reported that different kinds of flower pigments were synthesized in the exterior and calyx sides in *I. ochracea*, and that these two metabolites might be another type of anthocyanin [17]. They showed a relatively higher peak percent in the calyx side compared to the exterior part.

Although Yoshida et al. discussed that anthocyanins in petals remained unchanged before and after flowering [4], Lu et al. reported that glycosylation in anthocyanins changed during floral development in *I. purpurea* petals [10]. Our observation supported glycosylation of anthocyanins during flowering. Peaks from m/z 2000 to m/z 20000, considered to be ribosomal proteins, were not detected in MALDI biotyping in the initial analysis (data not shown). Morita et al. showed gene expression in petals and tubes in *I. nil* [18,19]. The changes of metabolites in BMG petal during floral development were considered as the results of biochemical reactions including gene expressions.

According to Figures 2 and 3 (Appendix Figure), all peaks obtained from the first to the fourth disc sample of one petal (within 2 cm of the exterior edge) showed almost the same values in peak percent scores. This suggested that metabolites in this 2 cm edge area were at almost the same concentration. When selecting petal parts for discrimination by MALDI biotyping using metabolites in the mass range between m/z 140–2000, the petal area within 2 cm from the outside edge should be used.

Conclusion

A sequential distribution analysis using disc samples from BMG petals showed a drastic change of metabolites during flowering. Thought the ultimate aim was to provide a rapid and costless discrimination of BMG varieties using petals, initial information for that purpose

was obtained by the sequential fingerprint distribution analysis of metabolites by MALDI-TOF MS.

Acknowledgements

We acknowledge Dr. J. Ishibashi for permission to use the MALDI-TOF MS apparatus.

References

1. Fukuda-Tanaka S, Inagaki Y, Yamaguchi T, Saito N, Iida S (2000) Color-enhancing protein in blue petals. *Specula morning glory blooms rely on a behind-the-sense proton exchanger. Nature* 407: 581.
2. Yoshida K, Kawachi M, Mori M, Maeshima M, Kondo M, et al. (2005) The involvement of tonoplast proton pumps and Na⁺(K⁺)/H⁺ exchangers in the change of petal color during flower opening of morning glory, *Ipomoea tricolor* cv. Heavenly Blue. *Plant Cell Physiol* 46: 407-415.
3. Yoshida K, Miki N, Mononoi K, Kawachi M, Katou K, et al. (2009) Synchrony between flower opening and petal-color change from red to blue in morning glory, *Ipomoea tricolor* cv. Heavenly Blue. *Proc Jpn Acad B* 85: 187-197.
4. Yoshida K, Mori M, Kondo T (2009) Blue flower color development by anthocyanins: from chemical structure to cell physiology. *Nat Prod Rep* 26: 884-915.
5. Hoshino A, Jayakumar V, Nitasaka E, Toyoda A, Noguchi H, et al. (2016) Genome sequence and analysis of the Japanese morning glory *Ipomoea nil*. *Nat Commun* 7: 13295.
6. Registration Kind Base.
7. Buchan BW, Ledebor NA (2014) Emerging technologies for the clinical microbiology laboratory. *Clin Microbiol Rev* 27: 783-822.
8. Kajiwara H (2016) Direct detection of the plant pathogens *Burkholderia glumae*, *Burkholderia gladioli* pv. *gladioli*, and *Erwinia chrysanthemi* pv. *zeae* in infected rice seedlings using matrix assisted laser desorption/ionization time-of-flight mass spectrometry. *J Microbiol Methods* 120: 1-6.
9. Kajiwara H, Hinamoto N, Gotoh T (2016) Mass fingerprint analysis of spider mites (Acari) by matrix-assisted laser desorption/ionization time-of-flight mass spectrometry for rapid discrimination. *Rapid Commun Mass Spectrom* 30: 1037-1042.
10. Lu Y, Du J, Tang JY, Wang F, Zhang J, et al. (2009) Environmental regulation of floral anthocyanin synthesis in *Ipomoea purpurea*. *Mol Ecol* 18: 3857-3871.
11. Harvey DJ (2015) Analysis of carbohydrates and glycoconjugates by matrix-assisted laser desorption/ionization imaging mass spectrometry: An update for 2009-2010. *Mass Spectrom Rev* 34: 268-422.
12. Zaima N, Goto-Inoue N, Hayasaka T, Setou M (2010) Application of imaging mass spectrometry for the analysis of *Oryza sativa* rice. *Rapid Commun Mass Spectrom* 24: 2723-2729.
13. Jung S, Chen YF, Sullards MC, Ragauskas AJ (2010) Direct analysis of cellulose in poplar stem by matrix assisted laser desorption/ionization imaging mass spectrometry. *Rapid Commun Mass Spectrom* 24: 3230-3236.
14. Lee YJ, Perdian DC, Song ZH, Yeung ES, Nikolau BJ (2012) Use of mass spectrometry for imaging metabolites in plants. *Plant J* 70: 81-95.
15. Perdian DC, Lee YJ (2010) Imaging MS methodology for more chemical information in less data acquisition time utilizing a hybrid linear ion trap-Orbitrap mass spectrometer. *Anal Chem* 82: 9393-9400.
16. Kondo T, Kawai T, Tamura H, Goto T (1987) Structure determination of heavenly blue anthocyanin, a complex monomeric anthocyanin from the morning glory *Ipomoea tricolor*, by means of the negative NOE method. *Tetrahedron Let* 28: 2273-2276.
17. Durbin M, Lundy KE, Morrell PL, Torres-Martinez CL, Clegg MT (2003) Genes that determine flower color: the role of regulatory changes in the evolution of phenotypic adaptations. *Mol Phylogenet Evol* 29: 507-518.
18. Morita Y, Hoshino A, Kikuchi Y, Okuhara H, Ono E, et al. (2005) Japanese morning glory dusky mutants displaying reddish-brown or purplish-gray flowers are deficient in a novel glycosylation enzyme for anthocyanin biosynthesis UDP-glucose: anthocyanidin 3-O-glycoside-2''-O-glycosyltransferase, due to 4-bp insertions in the gene. *Plant J* 42: 353-363.
19. Morita Y, Saitoh M, Hoshino A, Nitasaka E, Iida S (2006) Isolation of cDNAs for R2R3-MYB, bHLH and WDR transcriptional regulators and identification of c and ca mutations conferring white flowers in the Japanese morning glory. *Plant Cell Physiol* 47: 457-470.